PHYSICAL REVIEW B VOLUME 8, NUMBER 12 15 DECEMBER 1973

Calculation of Many-Body Effects on Energy Distribution Curves in Photoemission*

N. Tzoar and J. I. Gersten
Department of Physics, The City College of the City University of New York, New York, New York 10031
(Received 10 July 1973)

A study of the energy distribution curves of photoemitted electrons from the simple metals is made. Several mechanisms responsible for producing photoemitted electrons are considered. In addition to the usual surface-ejection mechanism, we investigate the emission produced by the imaginary optical potential. Processes involving bulk and surface plasmons are studied. The contribution to the spectrum of low-energy secondary electrons arising from plasmons is estimated.

I. INTRODUCTION

Following a long history of theoretical interest,[1] photoemission has recently emerged as a powerful tool for studying the properties of solids.[2] It has been demonstrated that the energy distribution curves (EDC's) of the photoemitted electrons are proportional (in some range) to the joint density of states of the solid. One regards the incident photon as inducing a direct transition from an occupied band to an unoccupied one. Thus valuable information concerning the band structure is obtainable from photoemission studies.

However, comparison of theory with experiment[3] shows that often this picture is applicable only to a small portion of the EDC. In the alkali metals, for example, this model would predict that the emitted electrons should lie in a narrow band of energies corresponding to the conduction-band Fermi sea displaced in energy by the photon energy minus the work function. In fact, electrons are observed with energies extending down to the vacuum level. Most of the photoemitted electrons do not even lie in the range defined by the direct transition model, but lie at lower energies.

The discrepancy has been traced to the important role played by many-body effects in the photoemission problem. Thus a proper treatment of the problem should include effects due to bulk plasmons, surface plasmons, and electron-hole pair production. This represents a rather formidable task from the many-body viewpoint because of the difficulty in carrying out the relevant integrations. The wave functions of the electrons near the surface of the crystal assume a complicated enough form to prevent sufficient progress to be made. For this reason a simplified approach to the many-body problem was developed[4] in which one could incorporate, in an approximate way, the effects of the above-cited elementary excitations. We will now apply this approach to photoemission.

In the present paper we will be interested in analyzing the EDC's of the alkali metals for ultraviolet-frequency photons. We take the simplest model that has been suggested—that of a step potential at the surface, and systematically add many-body effects to the problem. Our aim is twofold. First we wish to develop techniques for application to more sophisticated models.[5] Since such calculations will undoubtedly be numerical in nature, it is convenient to have an analytic model to use as a prototype. Such a model is provided by the one employed in this paper. Second, one can ask just how good is this simple model physically. As we shall see, the main features of the EDC's are explainable and the quantitative agreement is not unreasonable. The calculations are performed for potassium.

II. DIRECT PHOTOEMISSION

The quantum process responsible for photoemission has long been understood. An incident photon with energy $\hbar\omega$ and with negligibly small momentum is absorbed by an electron from the conduction band. In the absence of broken translational symmetry, the process would be forbidden since energy and momentum could not be simultaneously conserved. However, either because of the presence of the ion-core lattice or due to the transition between crystal and vacuum at the surface, translational invariance is broken. The electron, upon being promoted to an excited state above the vacuum level, is then capable of being registered as a photoemitted electron. The process just described will be called direct photoemission in contradistinction to processes in which the excited electron induces secondary excitations as it leaves the crystal. The present section will consider only the direct process.

This article is concerned with attempting to find a model for describing the EDC's of photoemitted electrons from the alkali metals. Before defining the model, it is worthwhile to discuss some elementary physical considerations. First it should be noted that the range of an electron which has absorbed an ultraviolet photon is not expected to exceed 5–10 Å. This is due to the fact that emission of surface plasmons, bulk plasmons, or excitation of electron-hole pairs form fairly competitive

channels with which elastic propagation of electrons must contend. Second, it should be noted that the pseudopotentials of the ion cores are expected to be rather weak, since the alkalis are, to a good approximation, free-electron-like metals. Both of these factors would tend to favor a situation in which the potential rise at the surface plays an important role in the photoemission process. On the other hand, one cannot neglect the fact that an ordered array of ion cores defines a set of Bragg directions which must be of importance in describing the angular distribution of the photoelectrons. One might argue, however, that if one were not observing the angular distributions, but rather were interested only in the gross energy distributions, that the existence of the Bragg directions might be overlooked, since one integrates over all angles. Thus, in the present paper, we will neglect the effect of the ion cores completely. We caution the reader, however, that if we find that we are able to explain quantitatively the EDC's, it points to the fact that they are insensitive to particular assumptions made about the crystal structure. Other experimental quantities, such as angular-resolved EDC's might not share this degree of agreement between theory and experiment.

The crystal is idealized as a potential well of depth V_0 and is assumed to have translational symmetry parallel to the surface. Thus

$$V(z) = -V_0\Theta(-z) , \tag{2.1}$$

where $\Theta(x)$ is unity for positive x and zero for negative x. Treating the system in the one-electron approximation, the single-particle unperturbed Hamiltonian may be written as

$$H_e = -\tfrac{1}{2}\nabla^2 + V(z) - iU(z,E) . \tag{2.2}$$

We are employing atomic units in which $\hbar = e = m = 1$. The optical potential has been denoted by $U(z,E)$ and takes into account real and virtual processes involving the emission and reabsorption of elementary excitations. In the previous paper[4] explicit expressions for the otpical potential have been derived. Let $|I\rangle$ denote the initial state of the electron and $|F\rangle$ the final state:

$$\begin{aligned} H_e|I\rangle &= E_I|I\rangle , \\ H_e|F\rangle &= E_F|F\rangle . \end{aligned} \tag{2.3}$$

In the presence of a radiation field the total Hamiltonian becomes

$$H = H_e + \alpha A_0\,\hat{\epsilon}\cdot\hat{p} = H_e + \alpha A_0\epsilon_z p_z . \tag{2.4}$$

Here $\alpha = 1/c$ is the fine-structure constant, A_0 is the strength of the vector potential associated with the incident light beam, and $\hat{\epsilon}$ is its polarization. Cognizance has been taken of the fact that only the component of the field perpendicular to the surface is capable of causing photoemission. In the dipole approximation the momentum of the photon is ignored.

Evaluation of the matrix element of the radiation term leads to

$$\begin{aligned} \langle F|H_\gamma|I\rangle = [\alpha A_0\epsilon_z/(E_F - E_I)] \\ \times[V_0\langle F|\delta(z)|I\rangle + \langle F|U_F p_z|I\rangle] . \end{aligned} \tag{2.5}$$

Here U_F denotes the optical potential evaluated at an energy E_F which is above the Fermi surface. Since the electron is initially below the Fermi surface where inelastic processes cannot occur, there is no corresponding term U_I. The first term in Eq. (2.5) is the conventional surface photoelectric term due to the potential rise at the surface. The second term arises from the fact that the optical potential is also capable of producing surface photoemission by virtue of its translational noninvariance. Stated simply, even if there were no real potential step at the surface but only a discontinuity in the dielectric properties, one would still obtain a surface photoelectric effect. The size of this effect relative to the conventional one is not negligible, since the magnitudes of V_0 and U_F are comparable. Alternatively, one can understand the origin of the second term as arising from the scattering associated with an absorption process. The momentum transfer involved in this scattering allows simultaneous energy and momentum conservation in the photoemission process.

An explicit formula for the initial state is found by solving the Schrödinger equation Eq. (2.3):

$$\begin{aligned} |I\rangle = e^{i\vec{p}_\perp\cdot\vec{r}}[\sqrt{\tfrac{1}{2}}(e^{ik_i z} + Re^{-ik_i z})\Theta(-z) \\ + De^{-k_i z}\Theta(z)] . \end{aligned} \tag{2.6}$$

Here $\vec{p}_\perp$ is the momentum of the initial state parallel to the surface. The propagation vector in the crystal is given by

$$k_i = [2(V_0 + \epsilon_i)]^{1/2} , \tag{2.7}$$

where $\epsilon_i = E_I - \frac{1}{2}p_\perp^2$ is the kinetic energy associated with z motion. In the vacuum region the attenuation constant is given by

$$k_i = (-2\epsilon_i)^{1/2} . \tag{2.8}$$

Two constants have been introduced and are defined by

$$D = ik_i\sqrt{2}\,/(ik_i - K_i) , \tag{2.9}$$

$$R = (ik_i + k_i)/(ik_i - K_i) . \tag{2.10}$$

A suitable model for the optical potential, $U_F(z)$, is provided by the optical potential step:

$$U_F = \gamma(E)\Theta(-z) . \tag{2.11}$$

The final state is given by

$$|F\rangle = e^{i\vec{p}_\perp\cdot\vec{r}}[Be^{ik_f^* z}\Theta(-z) + (e^{iq_F z}+Ae^{-iq_F z})\Theta(z)] . \quad (2.12)$$

This corresponds to a state which has unit outgoing amplitude into the vacuum and which is exponentially damped in the crystal. Here $\vec{p}_\perp'$ represents the component of the final momentum parallel to the surface. The propagation constants are given by

$$k_f = \{2[V_0+\epsilon_i+i\gamma(E_F)]\}^{1/2} , \quad (2.13)$$

and

$$q_f = (2\epsilon_f)^{1/2} . \quad (2.14)$$

The constants A and B are defined by

$$A = (q_f - k_f^*)/(q_f + k_f^*) , \quad (2.15)$$

$$B = 2q_f/(q_f + k_f^*) . \quad (2.16)$$

Evaluation of the matrix element is straightforward and leads to the expression

$$\langle F|H_\gamma|I\rangle = \frac{\alpha A_0 \epsilon_g i}{E_F - E_i}(2\pi)^2\delta^{(2)}(\vec{p}_\perp - \vec{p}_\perp')\left[V_0 B^* D + \frac{k_i B^*}{\sqrt{2}}\left(\frac{\gamma}{i(k_i-k_f)} + \frac{\gamma R}{i(k_i+k_f)}\right)\right] . \quad (2.17)$$

One notes that the z integrations have converged very nicely as $z \to -\infty$ since $\mathrm{Im}k_f > 0$. The emission rate is given by

$$\Gamma = 2\pi\int |\langle F|H_\gamma|I\rangle|^2 \Theta(E_F - W_F)\Theta(W_F - E_I)\delta(E_F - E_I - \omega)\delta(\epsilon - E_F)\frac{d^2p_\perp' dq_f}{(2\pi)^3}\frac{d^2p_\perp dk_i 2}{(2\pi)^3} . \quad (2.18)$$

Here we have calculated the rate for emitting electrons with energy $\mathcal{E}$: $\Gamma(\mathcal{E})d\mathcal{E}$ representing the number per unit time being produced with energy in the range $\mathcal{E}$ to $\mathcal{E}+d\mathcal{E}$. The Fermi factors have been introduced to keep the initial electron's energy below the Fermi level W_F, and the final electron's energy above the Fermi level. The range of q_f is over positive values only since negative q_f would mean that the electron goes into the crystal rather than out of it. Similarly, the range of k_i extends over positive values because these states lie in a nondegenerate portion of the z continuum. A factor of 2 is included to account for the two possible spin projections in the initial state.

The integrations over $\vec{p}_\perp$, $\vec{p}_\perp'$, and q_f may be performed and we find

$$\Gamma = \frac{1}{4\pi^2}\Theta(W_F+\omega-\mathcal{E})\int \frac{|\mathfrak{M}|^2}{[(\epsilon_i+\omega)(V_0+\epsilon_i)]^{1/2}}\, d\epsilon_i , \quad (2.19)$$

where

$$\mathfrak{M} = \langle F|H_\gamma|I\rangle/4\pi^2\delta^{(2)}(\vec{p}_\perp' - \vec{p}_\perp) , \quad (2.20)$$

and $\langle F|H_\gamma|I\rangle$ is given by Eq. (2.17). In the integral we take $\epsilon_f = \epsilon_i + \omega$. The range of integration is given by $\max(-v_0, -\omega) \leq \epsilon_i \leq \mathcal{E} - \omega$.

In order to compare theory with experiment it is convenient to calculate $\mathcal{Q}$, the number of electrons yielded per incident photon. Dividing by the incident photon flux

$$F = 2\omega^2 A_0^2/4\pi\hbar\omega c , \quad (2.21)$$

and taking into account the fact that the beam area is the projection of the surface area through the cosine of the angle of incidence θ, one obtains

$$\mathcal{Q} = 2\pi\Gamma/\omega\alpha A_0^2\cos\theta . \quad (2.22)$$

We note that $\mathcal{Q}\cos\theta/\sin^2\theta$ is independent of the angle, so this quantity will be the one that is actually computed. The formulas embodied in Eqs. (2.17), (2.19), (2.20), and (2.22) give the direct photoemission contribution to the EDC's.

In the direct photoemission process, electrons are elevated from their station in the conduction band by an energy ω. The resulting spectrum reflects, in a crude way, the joint density of states of the initial and final states. The energies of the emitted electrons range from $\hbar\omega - V_0$ to $\hbar\omega + W_F$ (W_F is defined by $W_F = -V_0 + \mathcal{E}_F$, where $\mathcal{E}_F$ is the Fermi energy). We now proceed to consider processes which result in lower-energy electrons being emitted.

III. PLASMON-ASSISTED PHOTOEMISSION

In this section we shall discuss processes in which the photoemitted electron is accompanied by an elementary excitation of the solid. These include bulk plasmons, surface plasmons, and electron-hole pairs. Other excitations, such as phonons, will be neglected as they lead to only a fine-structure perturbation relative to the above effects. In our previous paper[4] we developed a set of quasimode excitations whose character was that of bulk or surface plasmons at long wavelengths while at short wavelengths it portrayed the electron-hole excitations. Our goal will be to calculate the spectrum for the case where the ejected electron emits a bulk or surface quasimode excitation. Since these quasimode excitations are largely plasmon-like, we term such a process "plasmon-assisted photoemission".

The Hamiltonian to be considered now is the same as that of Eqs. (2.1) and (2.4) but with terms corresponding to the quasimode couplings and free quasimode fields added. Thus

$$H = -\tfrac{1}{2}\nabla^2 + V(z) - iU(z,E) + H_{\rm QM} + \alpha\vec{A}\cdot\vec{p} - \Phi\ , \tag{3.1}$$

where the free-quasimode Hamiltonian is

$$H_{\rm QM} = \sum_{\vec{k}} \omega_{\vec{k}} b_{\vec{k}}^{\dagger} b_{\vec{k}} + \sum_{\vec{k}_\perp} \sigma_{\vec{k}_\perp} a_{\vec{k}_\perp}^{\dagger} a_{\vec{k}_\perp}\ . \tag{3.2}$$

Here $\omega_{\vec{k}}$ is the frequency of the bulk quasimode (BQM) and $b_{\vec{k}}(b_{\vec{k}}^{\dagger})$ is the corresponding annihilation (creation) operator. The surface-quasimode frequency (SQM) has been denoted by $\sigma_{\vec{k}_\perp}$ and the corresponding annihilation (creation) operator by $a_{\vec{k}_\perp}(a_{\vec{k}_\perp}^{\dagger})$. The coupling to the quasimodes is given by an electrostatic coupling to the potential wave

$$\Phi = \frac{(2\pi)^3}{V_c}\sum_{\vec{k}}\left(M_{\vec{k}} b_{\vec{k}} \sin k_z z\,\Theta(-z) \times e^{i(\vec{k}_\perp\cdot\vec{r}-\omega_{\vec{k}}t)} + \text{H.c.}\right) + \frac{(2\pi)^2}{A}\sum_{\vec{k}_\perp}\left(N_{\vec{k}_\perp} a_{\vec{k}_\perp} e^{-k_\perp|z|} e^{i(\vec{k}_\perp\cdot\vec{r}-\sigma_{k_\perp}t)} + \text{H.c.}\right). \tag{3.3}$$

Perturbation theory will be employed and the radiation and quasimode coupling terms will be treated to first order in each. Higher-order effects in the quasimode fields are implicitly contained in U, the optical potential. Thus we will restrict our attention to final states in which there is only one quasimode excitation.

The Feynman diagrams for the plasmon-assisted photoemission amplitudes are given in Fig. 1(b). These are to be contrasted with the diagram for direct photoemission given in Fig. 1(a). We note that the absorption of the photon can either precede or follow the emission of the quasimode excitation, since the intermediate electron is off the energy shell. It can readily be shown that by summing over graphs in which the intermediate particle is either an electron or a hole, one obtains the simple perturbation formula in which Fermi-surface effects are neglected in the intermediate state.[6] The matrix element for quasimode (QM) -assisted photoemission is given by

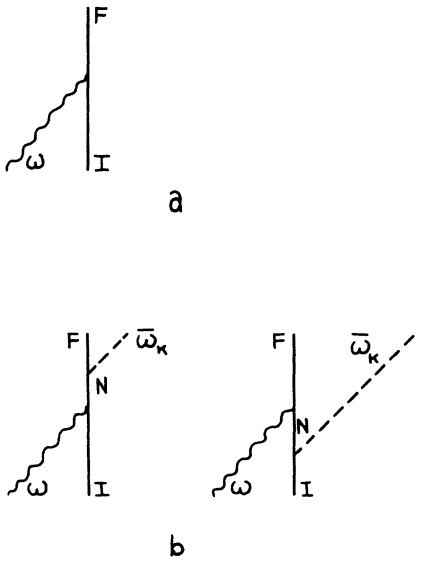

FIG. 1. (a) Feynman diagram for direct photoemission (b) Feynman diagrams for "plasmon-assisted photoemission."

$$M_{\rm QM} = \sum_N \left\{ \frac{\langle F|H_\gamma|N\rangle\langle N|H_{\rm QM}|I\rangle}{E_N - E_I - \bar{\omega}_k} + \frac{\langle F|H_{\rm QM}|N\rangle\langle N|H_\gamma|I\rangle}{E_N - E_I - \omega} \right\}. \tag{3.4}$$

Here we employ a condensed notation in which $\bar{\omega}_k$ represents ω_k (for BQM) or $\sigma_{k_\perp}$ (for SQM).

The rate for photoemission in which along with the emitted electron a quasimode of wave number k is produced is given by

$$\Gamma(\vec{k},\mathcal{E}) = 2\pi\sum_{IF}|\langle F|M|I\rangle|^2\Delta(E_F+\bar{\omega}_k-E_I-\omega) \times\delta(\mathcal{E}-E_F) f_I^{(-)} f_F^{(+)}\ . \tag{3.5}$$

One allows for lifetime broadening of the quasimodes by using a Lorentzian function:

$$\Delta(\epsilon) = (1/\pi)\,[D/(D^2+\epsilon^2)]\ , \tag{3.6}$$

rather than a δ function, where D is the decay rate of the quasimode. The appropriate Fermi factors have been denoted by $f_I^{(-)}$ and $f_F^{(+)}$. Since the emitted electron will automatically lie above the vacuum level, $f_F^{(+)} = 1$. Let us separate out the z dependence of the various states. Thus,

$$|F\rangle = e^{i\vec{p}_\perp\cdot\vec{r}}\varphi_f(z)\ ,$$
$$|I\rangle = e^{i\vec{p}_\perp\cdot\vec{r}}\varphi_i(z)\ , \tag{3.7}$$
$$M = e^{-\vec{k}_\perp\cdot\vec{r}}\mathfrak{M}\ .$$

Then we have

$$\langle F|M|I\rangle = (2\pi)^2\delta^{(2)}(\vec{p}_\perp' + \vec{k}_\perp - \vec{p}_\perp) \times\langle\varphi_f|\mathfrak{M}|\varphi_i\rangle\ . \tag{3.8}$$

One observes that the matrix element conserves only the two transverse momentum components—a reminder of the translational noninvariance of the problem. From Eqs. (3.4) and (3.8) one obtains

$$\langle\varphi_f|\mathfrak{M}|\varphi_i\rangle = \sum_n\left(\frac{\langle f|\phi^\dagger|n\rangle\langle n|H_\gamma|i\rangle}{\epsilon_i+\omega-\epsilon_n} \times\frac{\langle f|H_\gamma|n\rangle\langle n|\phi^\dagger|i\rangle}{\epsilon_f-\omega-\epsilon_n}\right). \tag{3.9}$$

We have taken the sum over intermediate states by making the replacement

$$\sum_N \to \sum_n \frac{d^2p_\perp^{(N)}}{(2\pi)^2}\ . \tag{3.10}$$

Let us introduce an auxiliary function $|u\rangle$ defined

as

$$|u\rangle \equiv \sum_n \frac{|n\rangle\langle n|H_\gamma|i\rangle}{\epsilon_i+\omega-\epsilon_n} , \tag{3.11a}$$

and a function $|v\rangle$:

$$\langle v| = \sum_n \frac{\langle f|H_\gamma|n\rangle\langle n|}{\epsilon_f-\omega-\epsilon_n} . \tag{3.11b}$$

Then u and v can be shown to satisfy the equations

$$\left(\epsilon_i+\omega-V(z)+iU+\frac{1}{2}\frac{d^2}{dz^2}\right)u = H_\gamma\varphi_i , \tag{3.12a}$$

and

$$\left(\epsilon_f-\omega-V(z)+\frac{1}{2}\frac{d^2}{dz^2}\right)v^* = H_\gamma\varphi_f^* . \tag{3.12b}$$

Then the matrix element of Eq. (3.9) can be written simply as

$$\langle\varphi_f|\mathfrak{M}|\varphi_i\rangle = \langle f|\phi^\dagger|u\rangle + \langle v|\phi^\dagger|i\rangle . \tag{3.13}$$

The first objective of the calculation is thus to obtain explicit expressions for the auxiliary functions u and v. Let

$$\begin{aligned} k_1 &\equiv [2(\epsilon_i+\omega+V_0+i\gamma)]^{1/2} , \\ q_1 &\equiv [2(\epsilon_i+\omega)]^{1/2} , \\ k_2 &\equiv [2(\epsilon_f-\omega+V_0)]^{1/2} , \\ q_2 &\equiv [2(\epsilon_f-\omega)]^{1/2} . \end{aligned} \tag{3.14}$$

The physical branch is the one in which both the real and imaginary parts of k_i and q_i are positive. Then inserting the explicit forms for the initial and final states given by Eqs. (2.6) and (2.12) into the differential equations Eqs. (3.12a) and (3.12b) and solving gives:

$$\begin{aligned} u = {} & (a_1 e^{ik_i z} + b_1 e^{-ik_i z} + c_1 e^{-ik_1 z})\Theta(-z) \\ & + (d_1 e^{-K_i z} + e_1 e^{iq_1 z})\Theta(z) , \end{aligned} \tag{3.15a}$$

and

$$\begin{aligned} v = {} & (a_2 e^{ik_f z} + b_2 e^{-ik_2 z})\Theta(-z) \\ & + (c_2 e^{-iq_f z} + d_2 e^{iq_f z} + e_2 e^{iq_2 z})\Theta(z) , \end{aligned} \tag{3.15b}$$

where

$$a_1 = \alpha\mathcal{E}_z A_0\sqrt{2}\,k_i/(k_1^2-k_i^2) , \tag{3.16a}$$

$$b_1 = -\alpha\mathcal{E}_z A_0\sqrt{2}\,Rk_i/(k_1^2-k_i^2) , \tag{3.16b}$$

$$d_1 = 2i\alpha\mathcal{E}_z A_0 TK_i/(K_i^2+q_1^2) , \tag{3.16c}$$

$$\begin{aligned} c_1 = {} & [(k_i-q_1)a_1 - (k_i+q_1)b_1 \\ & + (q_1-iK_i)d_1]/(k_1+q_1) , \end{aligned} \tag{3.16d}$$

$$e_1 = a_1+b_1+c_1-d_1 , \tag{3.16e}$$

and

$$a_2 = 2\alpha A_0\mathcal{E}_z Bk_f/(k_2^2-k_f^2) , \tag{3.17a}$$

$$c_2 = 2\alpha A_0\mathcal{E}_z Aq_f/(q_2^2-q_f^2) , \tag{3.17b}$$

$$d_2 = 2\alpha A_0\mathcal{E}_z q_f/(q_2^2-q_f^2) , \tag{3.17c}$$

$$\begin{aligned} b_2 = {} & [(k_f-q_2)a_2 + (q_f+q_2)c_2 \\ & + (q_2-q_f)d_2]/(k_2+q_2) , \end{aligned} \tag{3.17d}$$

$$e_2 = a_2+b_2-c_2-d_2 . \tag{3.17e}$$

Having found explicit formulas for u and v let us now proceed to calculate the matrix element of Eq. (3.13) for the two cases of interest—BQM and SQM emission. For BQM emission the interaction is[4]

$$\phi^\dagger = (2\pi)^3 M_k \sin k_z z\,\Theta(-z) , \tag{3.18}$$

with the coupling parameter given by

$$M_k = \omega_p/k(8\pi^5\omega_k)^{1/2} . \tag{3.19}$$

Hence we find

$$\begin{aligned} \langle f|\phi^\dagger|u\rangle = {} & -4\pi^3 M_k B^*\{a_1[(k_i+k_z-k_f^*)^{-1} - (k_i-k_z-k_f^*)^{-1}] \\ & + b_1[(-k_i+k_z-k_f^*)^{-1} - (-k_i-k_z-k_f^*)^{-1}] + c_1[(-k_1+k_z-k_f^*)^{-1} - (-k_1-k_z-k_f^*)^{-1}]\} , \end{aligned} \tag{3.20a}$$

and

$$\begin{aligned} \langle i|\phi|v\rangle = {} & -[(2\pi)^3/\sqrt{8}\,]M_k\{a_2[(k_f+k_z-k_i)^{-1} - (k_f-k_z-k_i)^{-1} + R^*(k_f+k_z+k_i)^{-1} - R^*(k_f-k_z+k_i)^{-1}] \\ & + b_2[(-k_2+k_z-k_i)^{-1} - (-k_2-k_z-k_i)^{-1} + R^*(-k_2+k_z+k_i)^{-1} - R^*(-k_2-k_z+k_i)^{-1}]\} . \end{aligned} \tag{3.20b}$$

Similarly, for SQM-assisted photoemission the interaction is[4]

$$\phi^\dagger = (2\pi)^2 N_{k_\perp} e^{-k_\perp|z|} , \tag{3.21}$$

with the coupling parameter given by

$$N_{k_\perp} = \omega_p/(32\pi^3 k_\perp\sigma_{k_\perp})^{1/2} . \tag{3.22}$$

Hence we find

$$\begin{aligned} \langle f|\phi^\dagger|u\rangle = {} & 4\pi^2 N_{k_\perp}\{B^*a_1[k_\perp+i(k_i-k_f^*)]^{-1} + b_1B^*[k_\perp-i(k_i+k_f^*)]^{-1} + c_1B^*[k_\perp-i(k_1+k_f^*)]^{-1} \\ & + d_1A^*[k_\perp+K_i-iq_f]^{-1} + d_1[k_\perp+K_i+iq_f]^{-1} + e_1A^*[k_\perp-i(q_1+q_f)]^{-1} + e_1[k_\perp-i(q_1-q_f)]^{-1}\} , \end{aligned} \tag{3.23a}$$

and

$$\langle i\,|\,\phi\,|\,v\rangle = 4\pi^2 N_{k_\perp}\{(a_2/\sqrt{2})[k_\perp + i(k_f - k_i)]^{-1} + (a_2 R^*/\sqrt{2})[k_\perp + i(k_i + k_f)]^{-1} + (b_2/\sqrt{2})[k_\perp - i(k_2 + k_i)]^{-1}$$
$$+ (b_2 R^*/\sqrt{2})[k_\perp - i(k_2 - k_i)]^{-1} + c_2 T^*[k_\perp + K_i + iq_f]^{-1} + d_2 T^*[k_\perp + K_i - iq_f]^{-1}$$
$$+ e_2 T^*[k_\perp + K_i - iq_2]^{-1}\}\ . \qquad (3.23b)$$

The rate for quasimode-assisted photoemission is given by Eq. (3.4):

$$\Gamma = 8\pi^2 \int \frac{d^2p_\perp\, dk_i z}{(2\pi)^3} \int \frac{d^2p_\perp'\, dq_f}{(2\pi)^3}\, \delta^{(2)}(\vec{p}_\perp' - \vec{p}_\perp - \vec{k}_\perp)\delta(\mathcal{E} - E_F)$$
$$\times \Theta(W_F - E_I)\Theta(\epsilon_i + V)\, \frac{D}{D^2 + (E_F - E_I + \sigma - \omega)^2}\, |\langle f\,|\,\phi^\dagger\,|\,u\rangle + \langle v\,|\,\phi^\dagger\,|\,i\rangle\,|^2\ . \qquad (3.24)$$

The integrations over $p_\perp'$ and ϕ (the angle between $k_\perp$ and $p_\perp$) may be readily performed, and this reduces to

$$\Gamma = (1/2\pi^4)\int dk_i\, dq_f\, \Theta(\epsilon_i + V)\,|\langle f\,|\,\phi^\dagger\,|\,u\rangle + \langle v\,|\,\phi^\dagger\,|\,i\rangle\,|^2 J\ , \qquad (3.25)$$

where we have let

$$J = D\int dx\, \frac{\Theta(W_F - \epsilon_i - x)\Theta[2k_\perp^2\chi - (\mathcal{E} - \epsilon_f - \frac{1}{2}k_\perp^2 - \chi)^2]}{[D^2 + (\mathcal{E} + \sigma - \omega - \epsilon_i - \chi)^2][2k_\perp^2 - (\mathcal{E} - \epsilon_f - \frac{1}{2}k_\perp^2 - \chi)^2]^{1/2}}\ . \qquad (3.26)$$

The integral J may be expressed in terms of the arcsine function. Thus the problem is reduced to a two-dimension integral which is performed numerically.

In order to evaluate the integral appearing in Eq. (3.26) we must know the damping rates for the quasimodes. The damping comes about, in the present model, by the excitation of electron-hole pairs. In Appendix A the decay rate for SQM's is computed, and in Appendix B the decay rate for BQM's is computed.

The contribution from plasmon-assisted processes to the EDC appear in an intermediate range of energies lying between $\omega - V_0 - \omega_k$ (or $\omega - V_0 - \sigma_{k_\perp}$) and $\omega + W_F - \omega_k$ (or $\omega + W_F - \sigma_{k_\perp}$). One can think of this feature as some sort of a distorted replica of the EDC produced by the direct photoemission process, but down shifted in energy by the frequency of the quasimode excitation. The actual number of electrons lying in this region is comparable to the number of direct photoemitted electrons, pointing to the fact that plasmon-assisted photoemission is by no means a small perturbation.

IV. SECONDARY ELECTRONS

The quasimode excitations that are produced in plasmon-assisted photoemission do not have an infinite lifetime but ultimately decay. The QM's are absorbed by an electron whose energy lies below the Fermi surface and this electron is promoted to an final state which might lie above the vacuum level. The electron can then leave the crystal and contribute to the EDC. We shall call such electrons secondary electrons. We note a similarity between the decay of a QM excitation and the direct photoemission process. In the latter case a transverse photon is absorbed while in the former case a longitudinal "photon" is absorbed. Whereas the transverse photon carries no momentum, however, the longitudinal one does.

If we were to give a strict quantum-mechanical derivation of the secondary spectrum then Feynman diagrams such as appear in Fig. 2(a) must be considered. The intermediate QM must be allowed to propagate off the energy shell and one must antisymmetrize the states F and F'. Such a calculation is very intricate, so to make the problem tractable several approximations are made. First of all we observe that the secondary electrons and primary electrons will often come out in different energy ranges, so that the exchange effect can be neglected in a first approxi-

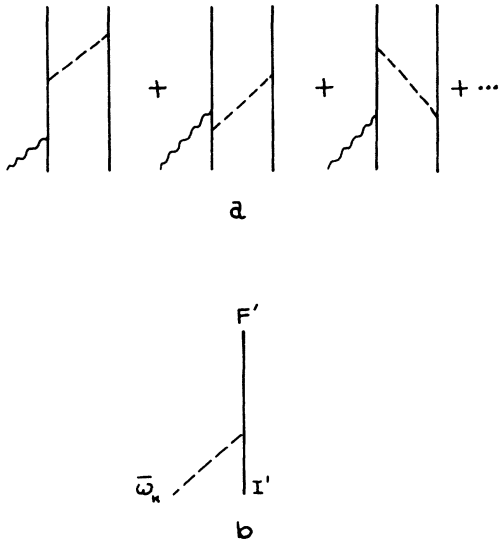

FIG. 2. (a) Feynman diagrams for secondary-electron production. (b) Feynman diagram for quasimode-excitation decay.

mation. Also, it is well known that the plasmons are fairly long lived since they are observed to have fairly narrow widths. Thus one might think of making a semiclassical calculation in which the production and decay mechanisms for plasmons are treated incoherently.

The Feynman diagrams for the production of QM excitations have already been given in Fig. 1(b). Rather than summing over the wave numbers corresponding to the quasimodes, one would sum over all states of the final electron, including those electrons which are emitted into the crystal. For high-energy electrons the number emitted into the crystal is roughly equal to the number emerging from the crystal. Let P_k denote the production rate for quasimode excitations characterized by wave numbers k. Let $D_k(\mathcal{E})$ denote the rate of decay of the QM in which electrons of energy $\mathcal{E}$ that emerge from the crystal are produced. The total decay rate of the QM will be denoted by D_k. If N_k denotes the number of quasimodes present at a given time, then

$$\frac{dN_k}{dt} = P_k - N_k D_k \,. \tag{4.1}$$

At equilibrium the net number of quasimodes is fixed, so

$$N_k = P_k / D_k \,. \tag{4.2}$$

Hence the net rate of production of photoemitted secondary electrons with energy $\mathcal{E}$ is

$$\Gamma_{\text{sec}}(\mathcal{E}) = \sum_{\vec{k}} \frac{P_k D_k(\mathcal{E})}{D_k} \,. \tag{4.3}$$

An assumption is being made that the QM excitation does not travel too far into the crystal before it decays. This does not weaken the argument too much for two reasons. First of all, the QM modes have very small group velocities, especially at long wavelengths where the couplings are strongest. Second, even if the QM excitation travels a modest distance into the crystal, the emitted electrons emerge with energies below the threshold for BQM emission, which means that they have very long mean free paths.

A crude approximation to $D_K(\mathcal{E})/D_K$ may be made by assuming that half the electrons produced in quasimode decay will leave the crystal. The spectrum is taken to be

$$\frac{D_k(\mathcal{E})}{D_k} = \frac{1}{2} \frac{\Theta(W_F + \sigma - \mathcal{E})}{W_F + \sigma} \,. \tag{4.4}$$

For all but very small wave numbers the full Fermi sphere is coupled by quasimode excitation to the vacuum states so the assumed spectrum is consistent with energy conservation. The assumption is undoubtedly an oversimplification since it ignores matrix elements effects. One might argue, however, that over the restricted range of energies involved in the quasimode decay spectrum, the matrix element variation may be omitted. A more serious objection to the above spectrum, perhaps, stems from the fact that it ignores possible constraints imposed by momentum conservation parallel to the surface. However, it should be noted that in realistic experiments, surface irregularities probably do much to lift the momentum conservation constraints. Consequently it is felt that Eq. (4.4) represents a plausible description of the decay spectrum. Thus we employ Eq. (4.4) and approximate the production spectrum by

$$P_k = 2 \int d\mathcal{E}\, \Gamma(\vec{k}, \mathcal{E}) \,, \tag{4.5}$$

where Γ is given in Eq. (3.5).

The electrons produced by the decay of the QM excitations are low-energy electrons. Their location is independent of the frequency of the incident radiation, unlike the case of direct photoemission or plasmon-assisted photoemission. The electrons range in energy up to the values $\mathcal{E} = W_F + \overline{\omega}_k$. The actual number of electrons in this spectral range is quite large, again attesting to the fact that the QM couplings are not weak. In fact, in some cases, the highest features of the spectrum are due to these secondary electrons.

V. RESULTS AND DISCUSSION

In Secs. I–IV we have considered various processes responsible for photoelectron emission. They were categorized as the direct process, the plasmon-assisted processes, and the secondary processes. In the direct process the photon elevates an electron from some place in the conduction band to a state above the vacuum level and the electron leaves the crystal. In the plasmon-assisted processes the same process occurs except either a SQM (surface-plasmon–like) or BQM (bulk-plasmon–like) excitation is also produced. Finally the secondary electrons are the decay products of these qasimode excitations. The list of processes we have considered is not exhaustive. It is quite possible that multiplasmon emission occurs and both the plasmon-assisted processes and secondary electron processes assoicated with it has been neglected.

In addition, the model chosen to describe the surface has been rather primitive. Ideally one would like to employ a realistic potential, such as has been proposed by Appelbaum and Hamann,[5] although it is clear that such a calculation would entail considerable labor. It should be emphasized, however, that the basic approach of the present paper is generalizeable to the case where the above approximations are not made. The goal of the present paper is to see how far one can go with the simple surface model and with the lowest-

order perturbation calculations. In particular we would like to study the many-body effects on the energy distribution curves.

Let us start by examining the direct photoemission process. As pointed out in Sec. II, this effect has two origins. The first is due to the momentum kick experienced by the electron at the surface due to the potential discontinuity. The second is due to the momentum components arising from the spatial dependence of the optical potential.

Calculations were performed for potassium, with the aim of comparing the theory with the experimental measurements of Smith and Spicer.[2] The photon energy was taken to be 11.2 eV. In the present calculation the plasmon (bulk) energy was taken to be 3.7 eV. The optical potentials corresponding to this plasma frequency have been given in the companion article.[4] The depth of the potential step is 4.4 eV and the work function is 2.3 eV. In Fig. 3 we present the quantity $\mathfrak{L}/\langle\sin^2\theta/\cos\theta\rangle$ as a function of energy $\mathcal{E}$. The energy scale is in units of the hartree (27.2 eV). Here $\mathfrak{L}$ is the number of photoelectrons per incident photon. The microscopic angle of incidence has been denoted by θ and is not known for this experiment. Thus all that we will really be able to compare are the relative shapes of the theoretical and experimental curves. That this should be the case can also be argued from consideration of our choice of the model. If it turned out that several atomic layers were responsible for the momentum kick received by the photoelectron prior to emission and we tried to ascribe it to a potential rise at the surface, it is clear that

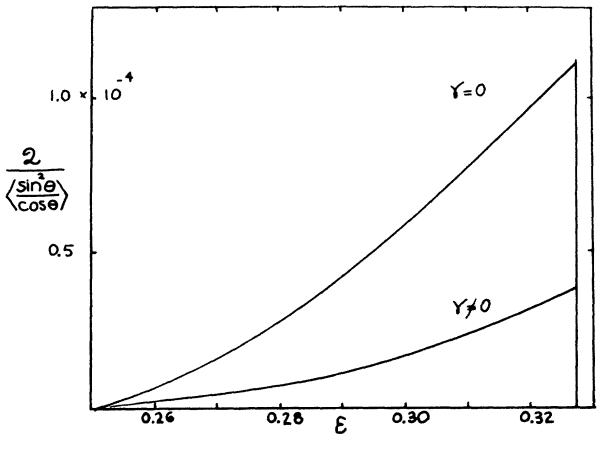

FIG. 3. Direct photoemission energy distribution curve. The abscissa is proportional to the number of electrons produced per incident photon. The energy $\mathcal{E}$ is in atomic units. Curves are shown for the cases with and without the optical parameter γ.

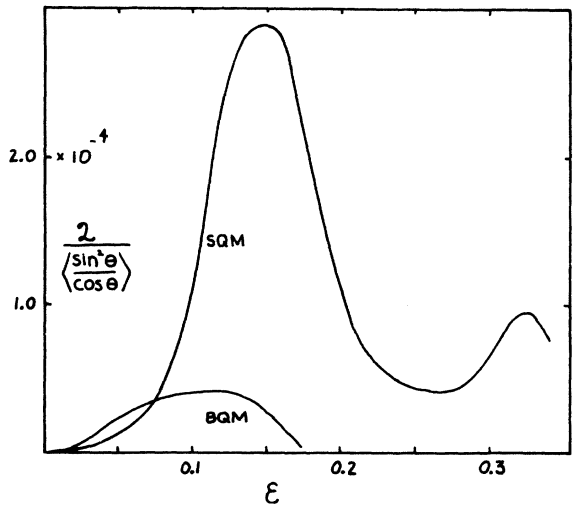

FIG. 4. Plasmon-assisted photoemission energy curves. The curve labeled BQM is due to bulk-quasimode excitation and that labeled SQM is due to surface-quasimode excitation.

the effective well depth V_0 might differ substantially from the sum of the Fermi energy and the work function. Thus, with our crude approximation, we are in no position to pin down the validity of the model to the point where quantitative agreement can be made. However, we expect quantities like $\sin^2\theta/\cos\theta$ to be on the order of unity for the alkali metals, so one should get order-of-magnitude or better agreement between theory and experiment.

Two curves are presented in Fig. 3 corresponding to direct photoemission with or without the bulk parameter γ. It is observed that there is a substantial change in the energy distribution curve upon introducing the optical potential—pointing to the sensitivity of these curves to the optical-potential parameters. One can understand the depression of the direct photoemission curve as resulting from a renormalization of the wave functions due to virtual quasimode excitation. Some intensity is sapped from the direct spectrum and is transferred to the quasimode-assisted spectra.

In Fig. 4 we present the EDC arising from the plasmon-assisted processes. The curve labeled SQM corresponds to photoemission in which a surface quasimode is emitted. We note that the coupling to the surface quasimode is considerably stronger. This could be understood by remembering that the surface quasimode is strongest at the surface and the bulk quasimode vanishes there. If the electron wave is substantially attenuated as one progresses into the crystal, then the coupling to the BQM excitations is expected to be weak.

A curious feature occurs in the quasimode-as-

sisted spectra at the high-energy end of the spectrum. It is observed that there is a secondary peak. The origin of this structure can be traced back to Eq. (3.5). One sees that the rate consists of a product of a phase-space factor and a matrix-element part. Since the phase space is essentially a joint density of states, it is a rapidly growing function of energy. The Lorentzian, on the other hand, has wings which only fall off inversely as the square of the energy. Thus it is possible that the joint-density-of-states factor can temporarily win out and give rise to a secondary peak. Unfortunately too much reliance cannot be put on the actual magnitude of this peak since, in all probability, one should employ a more rigorous line-shape theory. The location of this peak coincides with the location of the direct process peak and is slightly larger than it.

The secondary spectra arising from SQM and BQM decay have been added in Fig. 5. They appear as tall spikes at the low-energy end of the spectrum. Since there is more area under the SQM-assisted part of the spectrum of Fig. 4 it is logical that more electrons should appear under the SQM-decay spectrum.

Finally, in Fig. 6 the theoretical energy-distribution curve is presented (solid curve). The spectrum can be characterized as having a small bump at high energies, a bump at intermediate energies, and a high peak at lower energies. The highest-energy peak has its origin in two effects. First there is the direct photoemission process. Then there is the plasmon-assisted process in

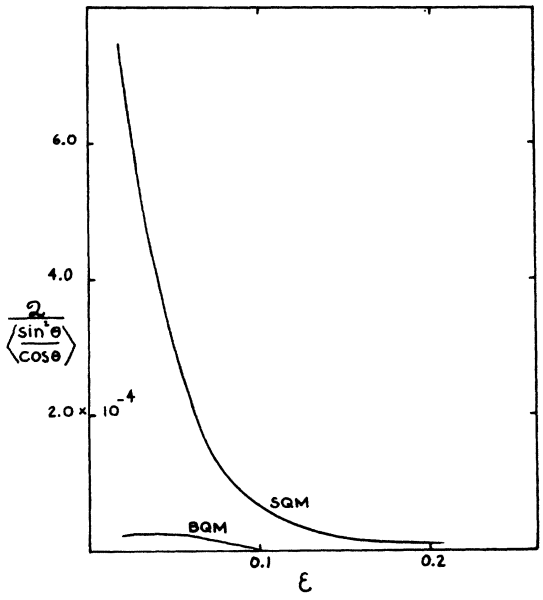

FIG. 5. Spectra resulting from quasimode decays.

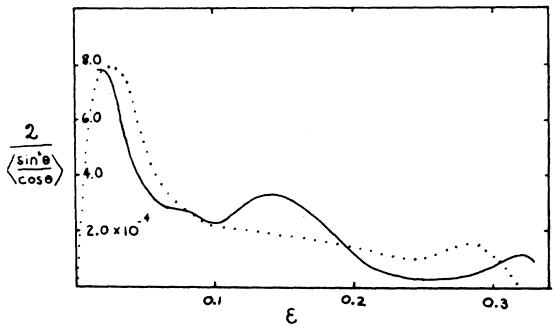

FIG. 6. Theoretical energy distribution curve (solid curve) and experimental curve (dotted curve).

which a secondary peak arises from the competition of the line shape and the phase space. The intermediate structure is due to the plasmon-assisted processes. Finally the low-energy structure stems from plasmon decay.

The experimental results of Smith and Spicer[2] are represented in Fig. 6 by the dotted curve. In order to bring the two curves into coincidence, the experimental data were multiplied by the numerical factor 2.56. Thus one can assign the surface roughness measure a value $\langle \sin^2\theta/\cos\theta \rangle = 1/2.56$. Again we caution against too literal a meaning to be given to this value since it assumes the effect to be dominated by surface photoemission.

Agreement between theory and experiment is reasonable, however, several observations must be made. First of all, the location of the high-energy peak seems to be displaced from the theoretical curve by about a volt. Presumably part of this can be ascribed to uncertainties in the Fermi energy and work function for the polycrystalline potassium.

The main discrepancy between theory and experiment occurs at intermediate energies. The experimental results are consistent with a model in which the surface plasmons are heavily damped, so as to wash out the structure associated with plasmon-assisted processes. In our calculation of the surface-plasmon lifetimes we have totally neglected surface roughness as a factor in contributing to the plasmon decay. Since experimental data, at present, does not provide us with a full characterization of the surface it does not appear possible to make a realistic calculation of plasmon lifetimes at this time.

In conclusion we see that even with rather crude assumptions, one is able to go a long way in describing the EDC's of photoemitted electrons from simple metals. Our results point to the dominant role played by electron correlation effects, such as plasmons and electron-hole pairs in determining the photoyield spectrum. Future investigations

will involve the use of a more realistic model of the solid to obtain accurate EDC's as well as angular-resolved photoemission curves.

APPENDIX A: DECAY RATE FOR SURFACE QUASIMODES

The decay of a surface quasimode is brought about by the creation of an electron-hole pair. The rate for this process is given by

$$D = 2\pi \sum_{IF} |\langle F|\Phi|I\rangle|^2 \times \delta(E_I + \sigma - E_F) f_I^{(-)} f_f^{(+)} . \quad \text{(A1)}$$

Here we concern ourselves with the second term of Eq. (3.3). As before, it is convenient to introduce an auxiliary function u defined by

$$|u\rangle = (E_I + \sigma + i\eta - H)^{-1}\Phi|I\rangle , \quad \text{(A2)}$$

where η is a small real number. Then, using the closure relation, one finds that

$$D = 2\eta \sum_I f_I^{(-)} \langle u|u\rangle , \quad \text{(A3)}$$

where the limit $\eta \to 0$ will ultimately be taken. If we let

$$|I\rangle = e^{i\vec{p}_\perp \cdot \vec{r}} \varphi_i(z) ,$$
$$\Phi = e^{i\vec{k}_\perp \cdot \vec{r}} \phi(z) ,$$
$$|u\rangle = e^{i\vec{p}_\perp \cdot \vec{r}} \chi(z) , \quad \text{(A4)}$$

then

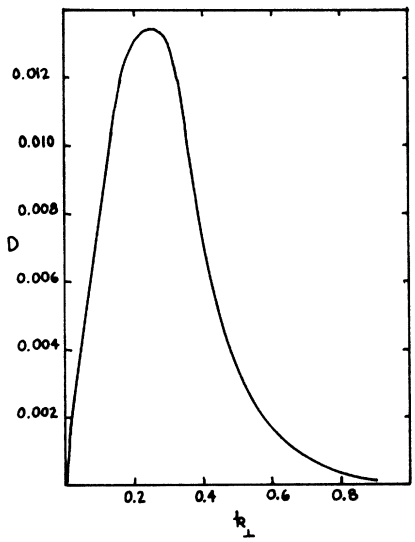

FIG. 7. Decay rate for surface quasimodes as a function of wave vector $k_\perp$.

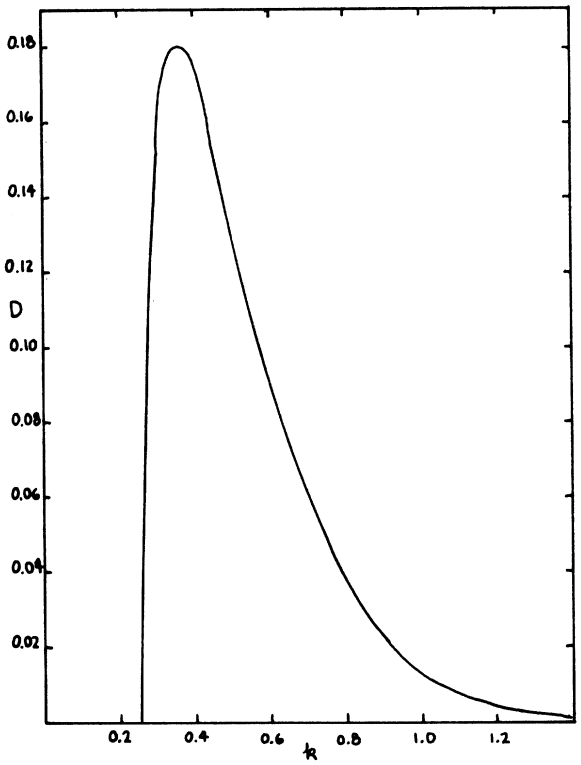

FIG. 8. Decay rate for bulk quasimodes as a function of wave vector k.

$$\left(\epsilon_i + \sigma - \vec{p}\cdot\vec{k}_\perp - \tfrac{1}{2}k_\perp^2 + \frac{1}{2}\frac{d^2}{dz^2} - V(z) + i\eta\right)\chi = \phi\varphi_i \quad \text{(A5)}$$

The solution to Eq. (A5) is

$$\chi = (a_1 e^{i(k_i - ik_\perp)z} + a_2 e^{-i(k_i + ik_\perp)z} + a_3 e^{-ikz})\Theta(-z) + (a_4 e^{-(K_i + k_\perp)z} + a_5 e^{iqz})\Theta(z) , \quad \text{(A6)}$$

where

$$k = [2(\epsilon_i + \sigma - \vec{p}_\perp \cdot \vec{k}_\perp - \tfrac{1}{2}k_\perp^2 + V_0 + i\eta)]^{1/2} ,$$
$$q = [2(\epsilon_i + \sigma - \vec{p}_\perp \cdot \vec{k}_\perp - \tfrac{1}{2}k_\perp^2 + i\eta)]^{1/2} , \quad \text{(A7)}$$

and the real and imaginary parts of k and q are positive. The constants are defined by

$$a_1 = (2\pi)^2 N\sqrt{2}\,[k^2 - (k_i - ik_\perp)^2]^{-1} ,$$
$$a_2 = (2\pi)^2 NR\sqrt{2}\,[k^2 - (k_i + ik_\perp)^2]^{-1} ,$$
$$a_4 = (2\pi)^2 N2T[q^2 + (K_i + k_\perp)^2]^{-1} , \quad \text{(A8)}$$
$$a_3 = [i(k+q)]^{-1}[a_1(k_\perp + i(k_i - q)) + a_2(k_\perp - i(k_i + q)) + a_4(K_i + k_\perp + iq)] ,$$
$$a_5 = a_1 + a_2 + a_3 - a_4 .$$

In the limit of small η it can readily be shown that

$$\lim_{\eta\to 0}\eta\langle u|u\rangle = \tfrac{1}{2}\left[|a_3|^2[2(\epsilon_i+\sigma-\vec{p}\cdot\vec{k}_\perp-\tfrac{1}{2}k_\perp^2+V_0)]^{1/2}\,\Theta(\epsilon_i+\sigma-\vec{p}\cdot\vec{k}_\perp-\tfrac{1}{2}k_\perp^2+V_0)\right.$$
$$\left.+\,|a_5|^2[2(\epsilon_i+\sigma-\vec{p}\cdot\vec{k}_\perp-\tfrac{1}{2}k_\perp^2)]^{1/2}\,\Theta(\epsilon_i+\sigma-\vec{p}\cdot\vec{k}_\perp-\tfrac{1}{2}k_\perp^2)\right]. \quad \text{(A9)}$$

So finally, we obtain

$$D=\frac{1}{2\pi^3}\int_0^{(2T_F)^{1/2}} dk_i \int_{-(2T_F-k_i^2)^{1/2}}^{+(2T_F-k_i^2)^{1/2}} dp_x\,(2T_F-k_i^2-p_x^2)^{1/2}$$
$$\times\left[k|a_3|^2\Theta(\epsilon_i+\sigma-p_xk_\perp-\tfrac{1}{2}k_\perp^2+V_0)+q|a_5|^2\Theta(\epsilon_i+\sigma-p_xk_\perp-\tfrac{1}{2}k_\perp^2)\right]. \quad \text{(A10)}$$

In the above expression T_F denotes the Fermi energy, i.e., $T_F = W_F + V$.

As we shall see, the decay arising from the above process is rather small, i.e., $D \ll \sigma_{k_\perp}$, thus justifying a calculation in which the decay rate is not calculated self-consistently. In Fig. 7 the decay rate for surface quasimodes as a function of wave vector parallel to the surface is presented. We note that damping occurs for all values of the wave vector but that it is maximum in the vicinity of the Fermi momentum.

APPENDIX B: DECAY RATE FOR BULK QUASIMODES

The bulk quasimodes decay by producing electron-hole pairs. Allowing for the possibility that the decay rate might be appreciable let us compute the decay rate self-consistently. Thus we have

$$D=2\pi\sum_{IF}|\langle F|\Phi|I\rangle|^2 f_I^{(-)} f_F^{(+)}\Delta(E_F-E_I-\omega_k)\,, \quad \text{(B1)}$$

where we employ a Lorentzian function

$$\Delta=\frac{1}{\pi}\,\frac{D}{D^2+(E_F-E_I-\omega_k)^2}\,. \quad \text{(B2)}$$

Here Φ is given by the first term of Eq. (3.3) corresponding to BQM annihilation. In the present calculation let us ignore the presence of the surface. This leads to errors at small k due to the fact that the decay can only occur there by virtue of the surface. However, once the quasimode has entered the region of k space defined by electron-hole processes the damping becomes strong and the surface is a small perturbation.

The integrations involved in evaluating Eq. (B1) are straightforward and lead to

$$D=\frac{(2\pi)^5}{\pi}\,\frac{|M_k|^2}{k}\int_{[2(T_F-\omega_k)]^{1/2}}^{(2T_F)^{1/2}} dp\,p$$
$$\times\left[\tan^{-1}\left(\frac{kp-\omega_k+\frac{1}{2}k^2}{D}\right)\right.$$
$$\left.+\tan^{-1}\left(\frac{kp+\omega_k-\frac{1}{2}k^2}{D}\right)\right]. \quad \text{(B3)}$$

This integral is expressible in terms of simple functions like the logarithm and arc tangent. A self-consistent numerical solution for D is sought.

In Figure 8 we present a graph of the decay rate for bulk quasimodes as a function of wave vector. The present curves exhibit a threshold behavior corresponding to the point where energy and momentum conservation become simultaneously possible in quasimode decay. In a more realistic calculation one would expect the decay rate to not exhibit this threshold behavior since the presence of the surface provides a momentum sink (or source). The actual self-consistent calculation of bulk-quasimode lifetimes in the presence of a surface is quite complicated and will not be discussed here. We only note that if the penetration of the plasmon into the solid is substantial (i.e. several atomic layers), then we should not expect the surface to have a very large effect on the decay properties and Fig. 8 is approximately correct.

*Research sponsored by the U.S. Air Force Office of Scientific Research, Air Force System Command, under AFOSR Grant No. 71-1978

[1]K. Mitchell, Proc. R. Soc. A **146,** 442 (1934); R. E. B. Makinson, Proc. R. Soc. A **162,** 367 (1937); Phys. Rev. **75,** 1908 (1949); H. Y. Fan, Phys. Rev. **68,** 43 (1945); M. J. Buckingham, Phys. Rev. **80,** 704 (1950); H. Mazer and H. Thomas, Z. Phys. **147,** 419 (1957); W. E. Spicer, Phys. Rev. **136,** A1030 (1964); I. Adawi, Phys. Rev. **134,** A788 (1964); Phys. Rev. **134,** A1649 (1964); J. J. Hopfield, Phys. Rev. **139,** A419 (1965); N. W. Aschcroft and W. L. Schaich, in *Proceedings of the Density of States Symposium* (U.S. GPO, Washington, D.C., 1969); L. Sutton, Phys. Rev. Lett. **24,** 386 (1970); thesis (Princeton University, 1970) (unpublished); S. Doniach and M. Sunjic, J. Phys. C 3, 285 (1970); S. Doniach, Phys. Rev. B 2, 3898 (1970); G. D. Mahan, Phys. Rev. B **2,** 4334 (1970); Phys. Rev. Lett. **24,** 1068 (1970); K. K. Thorbner, Phys. Lett. A **34,** 205 (1971); J. G. Endriz, Phys. Rev. B 7, 3464 (1973).

[2]N. V. Smith and W. E. Spicer, Phys. Rev. **188,** 593 (1969); N. V. Smith and G. B. Fisher, Phys. Rev. B **3,** 3663 (1971); D. E. Eastman and J. K. Cashion, Phys. Rev. Lett. **24,** 310 (1970); R. M. Broudy, Phys. Rev. B **3,** 3641 (1971); D. E. Eastman and W. D. Grobman, Phys. Rev. Lett. **28,** 1327 (1972); Phys. Rev. Lett. **28,** 1038 (1972); Phys. Rev. Lett. **28,** 1378 (1972); Phys. Rev. Lett. **28,** 1508 (1972).

[3]See N. V. Smith and W. E. Spicer, Ref. 2; N. V. Smith and G. B. Fisher, Ref. 2.

[4]J. I. Gersten and N. Tzoar, preceding paper, Phys. Rev. B 8, 5671 (1973).

[5]J. A. Appelbaum and D. R. Hamann, Phys. Rev. B **6,** 2166

(1972).

[6]The general equation for such a matrix element is

$$M_{QM} = -\sum_N f_I^{(-)} f_F^{(+)} \left[\langle F | H_{QM} | N \rangle \langle N | H_\gamma | I \rangle \times \left(-\frac{f_N^{(-)}}{-E_N + E_F + \bar{\omega}_k} + \frac{f_N^{(+)}}{-E_I + E_N - \omega} \right) \right.$$

$$\left. + \langle F | H_\gamma | N \rangle \langle N | H_{QM} | I \rangle \times \left(-\frac{f_N^{(-)}}{E_F - E_N - \omega} + \frac{f_N^{(+)}}{-E_I + \bar{\omega}_k + E_N} \right) \right].$$

Employing energy conservation $0 = E_F + \omega\bar{\omega}_k - E_I - \omega$, and the fact that $f_N^{(-)} + f_N^{(+)} = 1$, leads to the equation given below [Eq. (3.4)].